Inorganic Chemistry

Article

pubs.acs.org/IC

Nature of Zr-Monosubstituted Monomeric and Dimeric Polyoxometalates in Water Solution at Different pH Conditions: Static Density Functional Theory Calculations and Dynamic Simulations

Pablo Jiménez-Lozano,[†] Jorge J. Carbó,*[,†] Alain Chaumont,*[,‡] Josep M. Poblet,[†] Antonio Rodríguez-Fortea,[†] and Georges Wipff[‡]

[†]Departament de Química Física i Inorgànica, Universitat Rovira i Virgili, Campus Sescelades, Marcel·lí Domingo s/n, 43007 Tarragona, Spain

[‡]Laboratoire MSM, UMR CNRS 7177, Institute de Chimie, Universite de Strasbourg, 1, rue B. Pascal, 67000, Strasbourg, France

Supporting Information

ABSTRACT: Static density functional theory (DFT) calculations with a continuous solvent model as well as classical and Car−Parrinello molecular dynamics (MD) simulations with explicit solvent molecules were performed to study the nature of Zr-monosubstituted monomeric and dimeric polyoxometalates (POMs) in water at different pHs. We have analyzed Zr-aqua, -hydroxo, and -aqua-hydroxo species derived from Linqvist- and Keggin-type anions. Both DFT and Car−Parrinello MD methods suggest that the Zr center tends to have coordination number greater than 6 and can bind up to 3 water molecules. Car−Parrinello MD simulations also show that the Zr atom fluctuates within the oxide POM framework, providing a flexible coordination environment. There is a small thermodynamic preference for the Zr-aqua species over the protonated Zr-hydroxo species; however the prevalence of one or the other species might depend on the pH. Classical MD simulations show that H_3O^+ interacts mainly with hydroxo ligand, while OH^- anions prefer the protons of the H_2O ligands. In general, an increase of the acidity favors the formation of Zr-aqua species, explaining why dimer dissociation is promoted at low pH. At basic conditions Zr-hydroxo species are generated, providing the reactive groups to form Zr···Zr linkages.

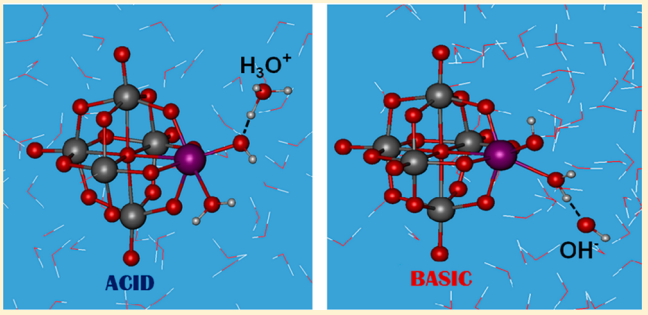

INTRODUCTION

Polyoxometalates (POMs) represent an important class of polynuclear metal−oxygen clusters composed mostly with Mo, W, and V elements plus sometimes other transition metals (TM).[1,2] Removal of a W═O unit from the complete structure results in a "lacunary" anion that has oxygen donor atoms available for bonding to other TM. This has allowed the preparation of a wide variety of POM derivatives by reaction of lacunary species of tungstopolyoxoanions with different metal ions including Ti^{IV}, Zr^{IV}, and Hf^{IV}. The chemistry of group IV metal-substituted POMs has shown potential applications in many fields such as catalysis, medicine, multifunctional materials; they can also serve as molecular analogues of TM single-site extended oxides.[3,4]

Group IV-containing POMs have a strong tendency to form intercluster linkages containing M-(μO)-M junctions when M = Ti, and M-(μOH)$_2$-M junctions when M = Zr, Hf (see Scheme 1).[3b] Moreover, the pH-dependent interconversion between dimeric and monomeric species of Zr/Hf-containing POMs has quite an opposite tendency from that of the group IV Ti-substituted POMs.[3b] For example, the dimeric form of

Scheme 1

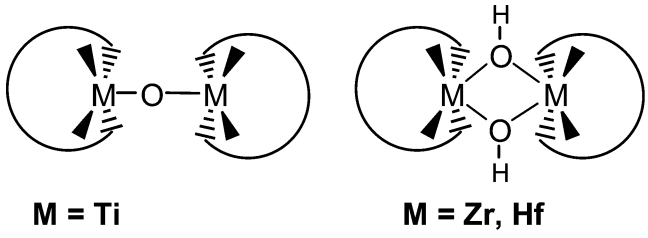

Ti-derivative of the Dawson ($P_2W_{17}Ti$) anion predominates under acidic conditions (pH 0.5−3.0), while the monomeric form is present at pH = 7.[3b,5] The reader should notice that often in POM chemistry anions are represented by a short-hand notation in which oxygen atoms and negative charge is not provided. Thus, for example, $P_2W_{17}Ti$ represents the anion $[P_2W_{17}TiO_{62}]^{8-}$. For Zr-derivative $P_2W_{17}Zr$, the dimeric species predominates at less acidic conditions (pH > 3.5),

Received: August 2, 2013
Published: December 24, 2013

   dx.doi.org/10.1021/ic401999r | *Inorg. Chem.* 2014, 53, 778−786

whereas the monomeric species is predominantly formed at more acidic conditions (pH < 3.5).[6] The differences in linkage type and coordination number have been related to the larger ionic radii of Zr and Hf atoms.[3b] These atoms do not fit so well in the vacancy of the lacunary anion.

The oligomeric Zr-containing polyoxotungstates have been prepared and isolated from both aqueous and nonaqueous solutions, and at different pH conditions. Villanneau et al. synthesized the first Zr-monosubstituted dimeric POM $[\{W_5O_{18}Zr(\mu\text{-}OH)\}_2]^{6-}$ (**2L**) in aqueous conditions by alkalination of the corresponding Zr-aqua Lindqvist monomers (**1L**).[7] The crystal structure $(TBA)_6[\{W_5O_{18}Zr(\mu\text{-}OH)\}_2]\cdot 2H_2O$ has two hydroxo bridges (Zr-$(OH)_2$-Zr) with seven-coordinated Zr atoms. Initially, the nature of the monomers was tentatively formulated as 6-fold coordinated Zr derivative $[W_5O_{18}Zr(H_2O)]^{2-}$.[7,8] But some years later, it was reformulated as a 8-fold coordinated Zr with three aqua ligands $[W_5O_{18}Zr(H_2O)_3]^{2-}$.[9] In nonaqueous conditions, Errington et al. synthesized a related methoxo-bridged dimeric Zr-monosubstituted Lindqvist-type POM $(TBA)_6[\{W_5O_{18}Zr(\mu\text{-}OMe)\}_2]$ that forms the corresponding hydroxide-bridged dimer **2L** by hydrolysis.[10] They also characterized a series of monomeric Lindqvist-type alkoxo derivatives, in which the coordination number of Zr is 6 or 7 depending apparently on the steric interactions between the alkoxo and the oxide cage.[10]

Using different synthetic and crystallization conditions, two groups obtained dimeric forms of the $PW_{11}Zr$ framework with different number of water ligands coordinated to the Zr^{IV} ion.[11,12] Kholdeeva et al.[11] used the "$H_5PW_{11}ZrO_{40}\cdot 14H_2O$" precursor and an excess of TBABr in acidic conditions, and obtained the $(TBA)_8[\{PW_{11}O_{39}Zr(\mu\text{-}OH)\}_2]$ compound, characterized by its X-ray structure in nonaqueous conditions. The synthesis by Nomiya et al.[12] used $[Zr(\alpha\text{-}PW_{11}O_{39})_2]^{10-}$ as precursor in HCl solution; in this case, crystallization performed in aqueous conditions yielded the X-ray structure with one coordinated water to each Zr atom $(Et_2NH_2)_8[\{PW_{11}O_{39}Zr(\mu\text{-}OH)(H_2O)\}_2]$. The two proposed structures also differ in their molecular symmetries, and in the interaction of Zr with the oxygen bound to the heteroatom. Other related Keggin-type dimers with aqua ligands, $[\{SiW_{11}O_{39}Zr(\mu\text{-}OH)(H_2O)\}_2]^{10-13}$ and $[\{PW_9O_{34}\{PO(R)\}_2\}_2\{Zr(\mu\text{-}OH)(H_2O)\}_2]^{4-}$,[14] have been also prepared.

Static density functional theory (DFT) calculations have analyzed the dimerization of monosubstitued-Lindqvist W_5M with (M = Ti, V, Nb, W, and Mo), and Keggin anions $PW_{11}M$ with (M = Nb and Ti), in acidic media via the formation of M-(μ-O)-M linkages.[15] In agreement with observations, calculations showed that dimerization is thermodynamically favored for Nb and Ti, while it is not for V, W, and Mo. For Zr derivatives, the doubly bridged hydroxo structure turned out to be thermodynamically more stable than the singly bridged oxo structure, in marked contrast with analogous Ti- and Nb-POMs.[11] In addition, this combined experimental-computational study indicated that protonation occurs preferentially at the Zr−O−Zr oxygens, and that acidic protons assist the interaction with water molecules to produce monomeric species, most likely $(TBA)_{3+n}[PW_{11}O_{39}Zr(OH)_n(H_2O)_{3-n}]$ (n = 0 and 1). Related calculations by Rustad et al. have focused on the oxygen exchange in Ti-substituted niobates[16] and Al polyoxocations,[17] studying proton affinities, hydronium-, water-, and hydroxide addition as a function of the structure and composition. In combination with kinetic experiments,[18] these studies allowed to determine the relative reactivities of the oxygen sites, its pH dependencies, and the local effect of Ti substitution.

Previous studies have shown that in general, the Zr center combines high coordination numbers and oxophilicity, flexible coordinated environments, and kinetically easy ligand exchange. These features make them attractive molecular platforms for tungstated zirconia catalyst development.[10] Experimentally, Zr-substitituted POMs showed varied coordination environments and structures, obtained with different synthetic procedures and at different conditions. Thus, assessing how the coordination of Zr ion varies as a function of the media is crucial to understand at the molecular level their reactivity and other properties. Valuable information on the behavior of POMs in solution can also be obtained from theoretical methods.[19] Here we use static DFT calculations and dynamics simulations (classical and Car−Parrinello molecular dynamics, MD) to investigate the reaction dynamics of Zr-substituted polyoxotungstates in solution, paying special attention to the dependence on the pH. In particular, we aim to understand dynamic processes such as protonation, water-, and hydroxide addition in both monomeric and dimeric Zr-substituted POMs.

METHODS

DFT Calculations. Static calculations were performed with the Gaussian09 package[20] at the DFT level by means of the hybrid exchange-correlation B3LYP functional.[21] For W and Zr atoms, the LANDL2DZ basis set was used.[22] The 6-31G(d,p) basis set[23] was used for H atoms, as well as for O atoms of hydroxo and aqua ligands and directly bound to Zr. For the remaining atoms we employed 6-31 G basis set.[23] Solvent effects were included in geometry optimizations by using ICE-PCM model[24] implemented in Gaussian09. The dielectric constant used to simulate aqueous solutions was ε = 78.35. Geometry optimizations of all structures were performed without any symmetry constraints.

Classical Molecular Dynamics (MD) Simulations. Classical MD simulations were performed to generate starting configurations for Car−Parrinello MD simulations, as well as to get some insight into the interaction between the Zr-substituted POMs and H_3O^+ or OH^- anions. We simulated three different systems mimicking acidic, neutral, and basic conditions (see Table 1). The size of the boxes was relatively small because of the high computational demand of Car−Parrinello MD simulations. Furthermore to keep the box sizes as small as possible we used Cs^+ as countercations instead of tetrabutylammonium cations which are used experimentally. Some of us have studied the role of counterions in bulk aqueous solutions of POMs.[25] Calculations revealed a marked counterion effect on POM anion aggregation, but we think that their role does not influence the coordination environment of the Zr atom which we will focus on in this study. The acidic and neutral systems were simulated with AMBER10[26] software while the basic system was simulated with AMBER11.[27] In both cases the potential energy U is described by a sum of bond, angle, and dihedral deformation energies and pairwise additive 1-6-12 (electrostatic and van der Waals) interaction between non bonded atoms; see eq 1:

Table 1. Characteristics of Simulated Aqueous Solutions

system	N_{H2O}	box size [Å^3]
$[W_5O_{18}Zr(OH)]^{3-} + 3H_3O^+$	131	16.3^3
$[W_5O_{18}Zr(OH)(H_2O)]^{3-} + 3Cs^+$	110	15.7^3
$[W_5O_{18}Zr(OH)(H_2O)]^{3-} + 3OH^- + 6Cs^+$	166	17.8^3

dx.doi.org/10.1021/ic401999r | Inorg. Chem. 2014, 53, 778−786

$$U = \sum_{\text{bonds}} k_b(b - b_0)^2 + \sum_{\text{angles}} k_\theta(\theta - \theta_0)^2 + \sum_{\text{dihedrals}} \sum_{n} V_n(1 + \cos(n\varphi - \gamma)) + \sum_{i<j} \left[\frac{q_i q_j}{R_{ij}} - 2\varepsilon_{ij}\left(\frac{R^*_{ij}}{R_{ij}}\right)^6 + \varepsilon_{ij}\left(\frac{R^*_{ij}}{R_{ij}}\right)^{12} \right] \quad (1)$$

Lorentz–Berthelot rules were used to construct the cross-terms in van der Waals interactions. The parameters for the Zr-substituted POMs and the OH^- anion were obtained following the procedure by Bonet-Avalos, Bo, Poblet et al.[28] We used CHELPG (charges from electrostatic potentials) atomic charges obtained from DFT-BP86/LANL2DZ calculations using Gaussian09 package on the optimized geometries at the BP86/TZV level[29] including the conductor-like screening model (COSMO)[30] to account for solvent effects. The geometry optimization was performed with the ADF2011 package.[31] The core potentials were generated with the DIRAC program using the scalar relativistic approach ZORA.[32] To build solvent cavity, the ionic radii were chosen to be 1.20, 1.52, 1.47, and 1.26 Å for H, O, Zr, and W atoms, respectively. The set of Lennard-Jones parameters for W and O atoms of the oxide POM framework were taken from previous work,[28] whereas those for Zr were taken from UFF force field.[33] The Cs^+ parameters were from Aqvist,[34] and the H_3O^+ parameters were from Wipff et al.[35]

Water was represented with the TIP3P model.[36] The 1-4 van der Waals and 1-4 Coulombic interactions were scaled down by 2.0. All simulations were done with 3D-periodic boundary conditions using an atom cutoff of 6 Å for nonbonded interactions and corrected for long-range electrostatic interactions by using the particle–particle mesh Ewald (PME) summation method.[37] The MD simulations were performed at 300 K starting with random velocities. The temperature was monitored by coupling the system to a thermal bath using the Berendsen algorithm[38] with a relaxation time of 0.2 ps. In the NPT simulations, the pressure was similary coupled to a barostat with a relaxation time of 0.2 ps. A time step of 1 fs was used to integrate the equation of motion via the Verlet leapfrog algorithm. After 500 steps of energy minimization, a 250 ps of dynamics were performed with fixed solutes (BELLY option of AMBER) to allow the solvent to somewhat relax around the solute. Then, dynamics of 250 ps at constant volume (NVT) followed by 500 ps at a constant pressure (NPT) of 1 atm were carried. Finally a production run of 1 ns at constant volume was performed.

Car–Parrinello Molecular Dynamics Simulations. The Car–Parrinello MD simulations were performed at the DFT level with the CPMD program package.[39] The electronic structure was described by expansion of the valence electronic wave functions into a plane-wave basis set, which is limited by an energy cutoff of 70 Ry. The interaction between the ionic cores and the valence electrons was treated through the pseudopotential (PP) approximation. Norm-conserving Martins-Troullier PPs were employed.[40] Nonlinear core corrections (NLCC)[41] were employed for W and Cs PP,[42] whereas for Zr a semicore PP was used. We adopted the generalized gradient-corrected BLYP exchange-correlation functional.[43] In the MD simulations, the wave functions were propagated in the Car–Parrinello scheme, by integrating the equations of motion derived from the Car–Parrinello Lagrangian.[44] We used a time step of 0.144 fs for the system at acidic conditions, whereas for neutral and basic systems the time step was shorter, 0.096 fs, because of integration problems. A fictitious electronic mass of 900 a.u was employed and H atoms were substituted by D atoms. The Nosé-Hoover[45] thermostat for the nuclear degrees of freedom was used to maintain the temperature constant around 300 K. Initial geometries for the simulations were created from equilibrated classical MD simulations of the same system (see above for details).

RESULTS AND DISCUSSION

We carried out DFT calculations to determine the geometries and energies of zirconium-aqua and -hydroxo derivatives of Lindqvist and Keggin anions, considering different hydrated and protonated forms of monomeric and dimeric species. For aqua species, optimization under water solvent effects via the continuum IEF-PCM model was required to obtain stable hydrated species. Beyond the simple static approach, we also performed Car–Parrinello MD simulations of a single monomeric Lindqvist species at different pH conditions to elucidate the coordination number of Zr and the nature of their ligands as a function of solution conditions.

DFT Calculations on Monomeric Structures. Table 2 lists the relative and hydration energies of monosubstituted

Table 2. Relative and "Hydration" Energies (in kcal mol^{-1}) for Zr-Monosubstituted POMs[a]

species	q	$E_{rel.}$	ΔE_{hydr}[b]	
		$n = 0$	$n = 1$	$n = 2$
Lindqvist (**1L**)				
aqua-$W_5Zr(H_2O)_{1+n}$	−2	0.0	−14.3	−28.2
hydroxo-$HW_5Zr(OH)(H_2O)_n$	−2	+2.3	−13.5	−22.9
dihydroxo-$H_2W_5Zr(OH)_2$	−2	+18.9		
hydroxo-$W_5Zr(OH)(H_2O)_n$	−3	0.0	−11.4	−17.5[c]
dihydroxo-$HW_5Zr(OH)_2$	−3	+12.3		
Keggin (**1K**)				
aqua-$PW_{11}Zr(H_2O)_{1+n}$	−3	0.0	−15.0	−27.3
hydroxo-$HPW_{11}Zr(OH)(H_2O)_n$	−3	+5.5	−12.3	−21.6
hydroxo-$PW_{11}Zr(OH)(H_2O)_n$	−4		−10.7	−19.8

[a]Relative energy, $E_{rel.}$ [b]"Hydration" energies, $\Delta E_{hydr.}$, defined by the reaction: [POM-$Zr(H_2O)$ or POM-$Zr(OH)$ + n H_2O → POM-$Zr(H_2O)_{1+n}$ or POM-$Zr(OH)(H_2O)_n$], for Zr-monosubstitued Lindqvist and Keggin anions. [c]Estimated value fixing the Zr–OH_2 and Zr–OH bond distances at their values in $[W_5O_{18}Zr(OH)(H_2O)]^{3-}$.

Linqvist anions (**1L**) $[W_5O_{18}Zr(H_2O)_{1+n}]^{2-}$, $[H_mW_5O_{18}Zr(OH)_m(H_2O)_n]^{2-}$, and $[W_5O_{18}Zr(OH)(H_2O)_n]^{3-}$ (m = 1, 2; and n = 0, 1, 2). Figure 1 shows the computed structures of

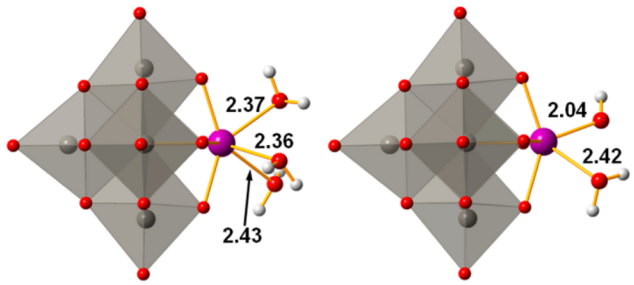

Figure 1. DFT structures and main distances (in Å) for Lindqvist-type Zr-aqua $[W_5O_{18}Zr(H_2O)_3]^{2-}$ (left) and Zr-hydroxo $[W_5O_{18}Zr(OH)(H_2O)]^{3-}$ (right) anions.

some relevant species. For the case of Zr-aqua anion $[W_5O_{18}Zr(H_2O)]^{2-}$, the successive coordination of a second and a third water is energetically favorable by 14.3 and 13.9 kcal mol^{-1}, respectively, in aqueous solution. This agrees with the proposal of Villanneau et al.[9] showing that the $\{W_5O_{18}Zr\}^{2-}$ moiety can link up to 3 water molecules to Zr reaching an 8-fold coordination. This coordination is achieved via the three O atoms of the water ligands, the four external O atoms of the lacuna, and the central O atom of the POM structure. It is worth noting that previous experimental[46] and theoretical[47]

dx.doi.org/10.1021/ic401999r | Inorg. Chem. 2014, 53, 778–786

studies reported a similar coordination number for the free Zr^{4+} in aqueous solution.

During geometry optimization of the dihydrated Zr-hydroxo species $[W_5O_{18}Zr(OH)(H_2O)_2]^{3-}$ one H_2O ligand dissociates from the Zr atom and moves to the second shell around the Zr atom where it forms hydrogen bonds with the hydroxo and the remaining aqua ligand, pointing to the fact that in the presence of a hydroxo ligand the 7 fold coordination is preferred over the 8 fold coordination. Moreover, the monohydration energy for hydroxo species (−11.4 kcal mol^{-1}) is less exothermic than that for the aqua (−14.3 kcal mol^{-1}).

It is difficult to compare directly the stability of Zr-hydroxo and -aqua species because of their different molecular charge. To compare like-charged species, we considered protonated hydroxo species $[HW_5O_{18}Zr(OH)(H_2O)_n]^{2-}$ with the proton at the bridging Zr−O−W oxygen, which is a more basic site than bridging W−O−W and terminal W═O oxygens in the TM(IV)-substituted POM framework.[11,15,48] The protonated Zr-hydroxo $[HW_5O_{18}Zr(OH)(H_2O)_n]^{2-}$ anions are higher in energy than the corresponding Zr-aqua anions $[W_5O_{18}Zr(H_2O)_{1+n}]^{2-}$ by 2.3, 3.1, and 7.6 kcal mol^{-1} for 6-, 7-, and 8-fold zirconium coordination, respectively. These energy differences are not too high suggesting that both species could coexist in different proportions, depending on the pH conditions. This issue will be analyzed in more detail by Car−Parrinello MD simulations (see below), but we can already observe some trends. As mentioned above, the protonation at the terminal hydroxo oxygen is energetically preferred over protonation at the bridging Zr−O−W oxygen. Moreover, as the number of protons in the complex increases, the Zr atom becomes more electrophilic, and it binds more effectively nucleophilic aqua ligands. For $[HW_5O_{18}Zr(OH)]^{2-}$, the first and second water coordination energies are −13.5 and −9.4 kcal mol^{-1}, whereas for the less electrophilic $[W_5O_{18}Zr(OH)]^{3-}$ anion, the first water coordination energy is −11.4 kcal mol^{-1} and the second is not stable. Additionally, we optimized the Zr-dihydroxo species but they turned out to be significantly higher in energy than their corresponding Zr-monohydroxo and -aqua species. The $[H_2W_5O_{18}Zr(OH)_2]^{2-}$ and $[HW_5O_{18}Zr(OH)_2]^{3-}$ anions are 15.7 and 12.3 kcal mol^{-1} higher in energy than the Zr-monohydroxo $[HW_5O_{18}Zr(OH)(H_2O)]^{2-}$ and $[W_5O_{18}Zr(OH)(H_2O)]^{3-}$ anions. Therefore, we propose that the formation of dihydroxo species is less likely.

For the corresponding Zr-monosubstituted Keggin anions (**1K**), we found similar trends (see Table 2). The Zr center can coordinate up to three water molecules. Furthermore, the Zr-hydroxo species have less tendency to bind additional aqua ligands than Zr-aqua. The first coordination energies are −11 and −15 kcal mol^{-1} for the $[PW_{11}O_{39}Zr(OH)]^{4-}$ and $[PW_{11}O_{39}Zr(H_2O)]^{3-}$ anions, respectively. Although in this case the dihydrated Zr-hydroxo species are stable, the $[HPW_{11}O_{39}Zr(OH)(H_2O)_2]^{3-}$ anion is significantly higher in energy (11.2 kcal mol^{-1}) than the Zr-aqua $[PW_{11}O_{39}Zr(H_2O)_3]^{3-}$ anion. Thus, static DFT calculations indicate that the most stable species are the trihydrated and the hydroxo-monohydrated zirconium POMs.

Molecular Dynamic Simulations on Monomeric Structures. To obtain a more reliable description of Zr coordination in solution, explicit representation of counterions and water molecules is required.[49,50] To this end, we performed Car−Parrinello MD simulations on aqua-hydroxo Zr-mono-substituted Lindqvist anions in water solution. Initially, we equilibrated the systems using classical MD simulations. Then, we selected configurations where the H_3O^+ or OH^- ions are close to the Zr−OH or Zr−H_2O moieties as starting points for Car−Parrinello MD simulations. Both in acidic[11] and basic[7] media, the observed dimerization might involve Zr-hydroxo intermediates, in the latter case via deprotonation of aqua ligands. Therefore, we simulated Zr-hydroxo anions $[W_5O_{18}Zr(OH)(H_2O)_n]^{3-}$ (n = 0, 1) at different pH conditions.

First, we simulated the behavior of a low-coordinated 6-fold zirconium at high acidic conditions (Table 1, first row).[51] Initial classical MD simulations gave some insight into the interactions between $[W_5O_{18}Zr(OH)]^{3-}$ anions and H_3O^+ cations. We calculated the average distribution of H_3O^+ by the radial distribution function (RDF) around the central oxygen (O_c) of the POM. The $O_c\cdots O(H_3O^+)$ RDF shows a broad peak between about 5.0 and 7.0 Å that integrates 1.4 H_3O^+ (see Supporting Information). A more detailed analysis of H_3O^+ interaction with hydroxo oxygen (O_h), terminal oxygens (O_t), bridging Zr−O−W (O_b) oxygens, and W−O−W oxygens ($O_{b'}$) shows that the H_3O^+ protons mainly interact with O_h. In the $O_h\cdots H(H_3O^+)$ RDF, we observed two sharp peaks at 1.6 and 2.9 Å, which integrate to 1 and 2 H atoms. These results indicate the formation of a strong hydrogen bond between one H atom of H_3O^+ and the hydroxo oxygen, while the other protons of H_3O^+ sit at longer distance. There is no significant peak below 3 Å around bridging oxygen atoms, and only small peaks around the terminal oxygens. This indicates that H_3O^+ cations do not form permanent hydrogen-bonds with the POM framework. Figure 2 depicts the high density regions of surrounding $O(H_3O^+)$ atoms, where the highest cation condensation is observed around the Zr-hydroxo moiety.

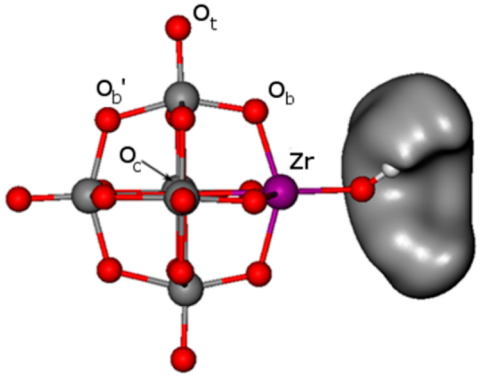

Figure 2. $[W_5O_{18}Zr(OH)]^{3-}$ anion with high density of the $O(H_3O^+)$ atoms (gray). Averages taken over the equilibrated 1 ns of classical dynamics.

Figure 3 shows a snapshot of the Car−Parrinello MD simulated structure and the evolution of selected distances along the trajectory. The first observed event is the coordination of a water molecule from the solvent to the 6-coordinated Zr (the Zr−O_w distance between 2.20 and 2.45 Å), indicating that in aqueous solution the Zr will increase its coordination number. Also at the beginning of the simulation, one proton transfers from H_3O^+ to the oxygen of Zr−OH group forming diaqua Zr-POM. Because of the short simulation time required for observing protonation, we can conclude that the corresponding energy barrier is low. The Zr-diaqua complex lasted for the rest of the simulation, but we cannot discard the coordination of a third water molecule at longer time scales. Thus in aqueous solutions, the six-coordinated

dx.doi.org/10.1021/ic401999r | Inorg. Chem. 2014, 53, 778−786

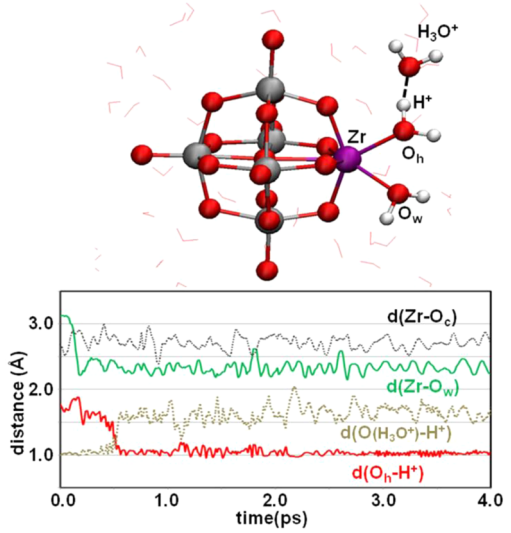

Figure 3. Selected Zr−O and O−H(H_3O^+) distance evolutions (in Å) for the 4 ps Car−Parrinello MD simulation at acidic conditions starting from Zr-hydroxo $[W_5O_{18}Zr(OH)]^{3-}$ anion, finally forming the seven-coordinated Zr species shown on top.

hydroxo species is unlikely to be observed since the Zr center tends to increases its coordination number to 7 or 8. This supports the reformulation by Villanneau et al. of the Zr-monosubstituted anion as a 8-fold Zr-triaqua structure, $[W_5O_{18}Zr(H_2O)_3]^{2-}$.[9] Moreover, the results are in line with static DFT calculations predicting that protonation to form a Zr-diaqua species is thermodynamically favored over the protonation at W−O−Zr oxygen to yield Zr-hydroxo-aqua species. Also, the monomeric hydrated Zr^{4+} ion has been reported to predominate at strongly acidic conditions.[46]

Interestingly, we noted that under very acidic conditions (pH < 3.5), the monomeric Dawson POMs, $[\alpha_2\text{-}P_2W_{17}O_{61}Zr(H_2O)_3]^{6-}$, are predominantly formed, whereas under less acidic conditions (pH > 3.5) dimeric Dawson POMs are predominant.[6] A similar phenomenon is observed for Keggin species.[11] Our simulations show that in acidic conditions, there is a tendency to protonate hydroxo ligands yielding aqua ligands that would not be suitable to form intercluster Zr···Zr linkages. Accordantly, previous studies on dimer cluster $[Zr_2(\mu\text{-}H_2O)(\mu\text{-}OH)(H_2O)_{12}]^{7+}$ proved that the H_2O bridge is unstable and departed in the course of the in vacuum CPMD simulation.[52] Finally, we expect that the new insight into the aqueous solution behavior of Lindqvist anion can be extended to the larger Keggin and Wells-Dawson anions because the experimental and DFT similarities.

Second, to investigate the stability of hydroxo species at higher pHs, we performed another Car−Parrinello MD simulation of the $[ZrW_5O_{18}(OH)(H_2O)]^{3-}$ anion in aqueous solution at neutral pH (Table 1, second row). In this case, we observed neither protonation of the hydroxo ligand nor coordination of an additional water molecule to Zr. Although aqua ligands around the free Zr^{4+} ion have a strong tendency to hydrolyze and its fully hydrated form only exists in extremely acidic conditions,[46] we did not observe the deprotonation of the aqua ligand in the case of the $[ZrW_5O_{18}(OH)(H_2O)]^{3-}$ anion. In a previous 10 ps simulation no hydrolysis reaction occurred for Zr^{4+} ion in aqueous solution at room temperature but at higher temperatures (>600 K), suggesting that hydrolysis would have occurred if longer simulation times were available.[47]

Here, for the $[ZrW_5O_{18}(OH)(H_2O)]^{3-}$ anion, we expect significantly less tendency toward further hydrolysis because ligands of the Zr center are already partially hydrolyzed. Moreover, when Zr^{4+} ions are incorporated into a POM structure its hydrolyzing capability seems to diminish since for Dawson structures of the triaqua species exist up to pH = 3.5. Thus, all these results indicate that Zr-hydro-aqua species are kinetically stable at moderate pHs provided that no dimerizations occur.

The simulation reflects the larger flexibility of the Zr−OH_2 bond (Zr−O_w = 2.14−2.66 Å) with respect to the Zr-hydroxo one (Zr−O_h = 1.95−2.26 Å). The Zr−O RDF and its integration can yield the Zr−O coordination number as Figure 4 displays. The relatively broad peak about 2.0−2.6 Å that

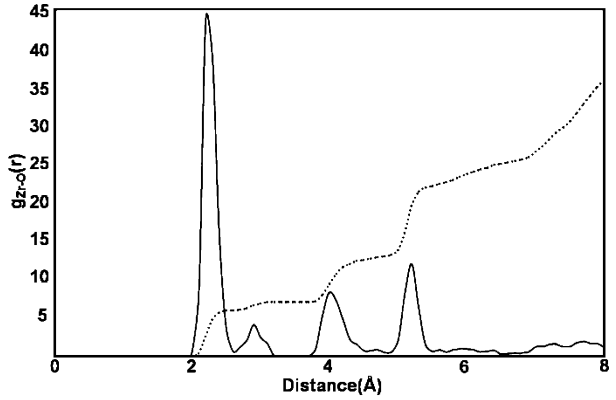

Figure 4. Zr−O RDF (solid line) and its integration (broken line) computed for 4 ps of Car−Parrinello MD simulation starting from $[W_5O_{18}Zr(H_2O)(OH)]^{3-}$ anion.

integrates six O atoms can be attributed to the aqua, hydroxo ligand, and the four external oxygens of the lacunary site of the POM framework. The spike at around 2.9 Å that integrates one more O atom corresponds to the central oxygen O_c. This peak is quite broad about 2.7−3.2 Å, indicating that the position of Zr atom is relatively loose within the POM framework. The Zr−O_c distance varies from 2.56 to 3.07 Å, which is significantly larger and wider than the W−O_c bond distances (from 2.18 to 2.57 Å). As already discussed,[4] the Zr atom does not fit well into the monolacunary site of the POM and, therefore, it is displaced away from the POM surface. On going from soft aqua to hard hydroxo ligands, this trend becomes more pronounced: Zr−O_c = 2.40−2.97, 2.56−3.07, and 2.71−3.15 Å, respectively for Zr-diaqua, -aqua-hydroxo, and dihydroxo species (simulations below and above).

Third, we simulated the behavior of the $[ZrW_5O_{18}(OH)(H_2O)]^{3-}$ anion at high basic conditions (Table 1, last row).[51] During the classical MD simulation, we observed short-life contacts (10−50 ps) between Zr−H_2O hydrogens and the OH^- ion. The H_w···O(OH^-) RDF shows a peak at 1.65 Å, that integrates to 0.05 OH^- only. We used one of these geometries as starting point for Car−Parrinello MD simulation. Figure 5 shows a typical snapshot of the Car−Parrinello MD simulation and the evolution of selected distances along the trajectory. At the beginning of the simulation, one proton of the aqua ligand is transferred to a hydroxide anion forming the dihydroxo $[W_5O_{18}Zr(OH)_2]^{4-}$ species, whereas the resulting H_2O molecule remains hydrogen-bonded to the hydroxo ligand. This new species stays stable during all the simulation. Our results resonate with pioneering work by Rustad on dynamic

dx.doi.org/10.1021/ic401999r | Inorg. Chem. 2014, 53, 778−786

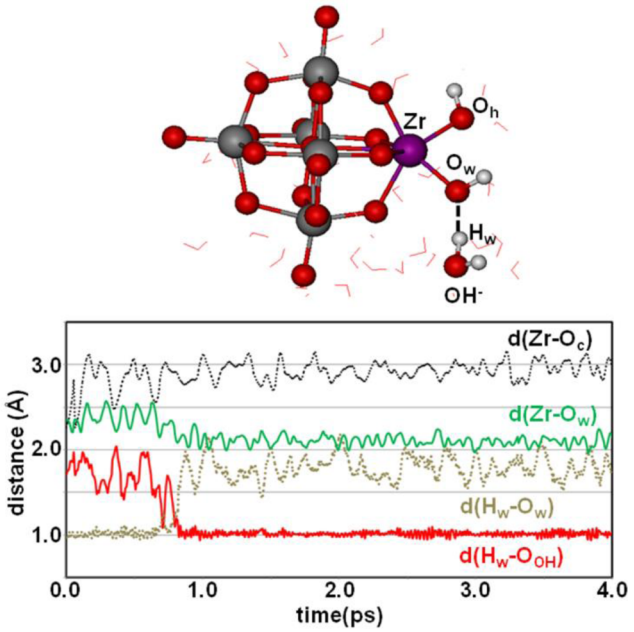

Figure 5. Selected Zr−O and (aqua)H_w-O distance evolutions (in Å) for the 4 ps Car−Parrinello MD simulation at basic conditions starting from Zr-aqua-hydroxo $[W_5O_{18}Zr(H_2O)(OH)]^{3-}$ anion. The geometry of the Zr species along with the nearest water molecules that solvate the Zr moiety.

simulations of titration with hydroxide ions.[17b] For aluminum polyoxocations, the author found that the η-H_2O ligands deprotonate forming a $H_3O_2^-$ ligand by pairing with the bound water.

Hence, the Zr-hydroxo species becomes more favorable at basic conditions. This is alike to the proposal of Villanneau et al.,[7] according to which the addition of alkalinization agent is required to deprotonate the aqua ligand and to form the reactive hydroxo species for dimerization. Moreover, as DFT calculations show, the bridging Zr−O−W oxygen is not basic enough to deprotonate aqua ligands. Rustad and Casey have shown that hydroxide addition can lead to metastable configurations of Ti-substituted niobates that are involved in oxygen exchange reactions.[16] This process may be also involved in the decomposition of POMs at high basic conditions. Here, although simulations correspond to very high pH values,[51] we do not observe such a process. Probably, in the simulated time scale, only fast events such as proton transfer occur. Nevertheless, as described above, the hydroxo ligands favor the displacement of the Zr away from the POM surface that could promote dissociative pathways through this local site.

In summary, our simulations on monomeric Zr-POMs show that in aqueous conditions the Zr^{IV} ion of substituted Lindqvist increases its coordination number (7- or 8-fold) by binding additional water molecules. When moving to high acidic conditions the Zr-aqua species are favored, whereas increasing the pH the hydroxo species becomes more accessible. This would explain why at high acid conditions (pH < 3.5) the monomeric species predominate for Dawson structures,[6] and why alkali promotes dimer formation. It is reasonable to think that hydroxo groups are required to form μ-OH linkages,whereas the aqua groups are unavailable to act as bridging ligands without further proton transfer.

DFT Calculations on Dimeric Structures. We also studied the hydration of dimeric Lindqvist $[\{W_5O_{18}Zr(\mu\text{-}OH)\}_2]^{6-}$ (**2L**) and Keggin $[\{PW_{11}O_{39}Zr(\mu\text{-}OH)\}_2]^{8-}$ (**2K**) species, using as starting point the X-ray determined structures.[7,10−12] The coordination of one water molecule for each Zr atom to yield $[\{W_5O_{18}Zr(H_2O)_2(\mu\text{-}OH)\}_2]^{6-}$ (**2L-2H$_2$O**) and $[\{PW_{11}O_{39}Zr(H_2O)_2(\mu\text{-}OH)\}_2]^{8-}$ (**2K-2H$_2$O**) is energetically favorable by 21.6 and 22.2 kcal mol^{-1}, respectively, in PCM-water. The values are similar to those of the monomers.

To analyze in more detail the water coordination, we divided the hydration energy (ΔE_{hydr}) into interaction (ΔE_{int}) and distortion (ΔE_{dist}) terms.[53] The ΔE_{dist} is defined as the energy cost to bring the fragments from their free geometries to those they adopt in the final structure. Although the relative disposition of the two Lindqvist- and Keggin-type subunits change significantly upon water coordination (see Figures 6 and 7), the computed ΔE_{dist} for the dimeric fragments are not very high, 16.1 and 15.5 kcal mol^{-1}, pointing out that Zr centers act as flexible hinges allowing the flapping of the POM scaffolds. All computed dimerization energies (ΔE_{dim}) are found to be exothermic by −25.0, −23.9, −22.8, −23.6 kcal mol^{-1} for **2L**, **2L-H$_2$O**, **2K**, and **2K−H$_2$O**, respectively [2 $Zr(H_2O)_nOH \rightarrow \{Zr(H_2O)_n(\mu\text{-}OH)\}_2$ n= 0, 1].

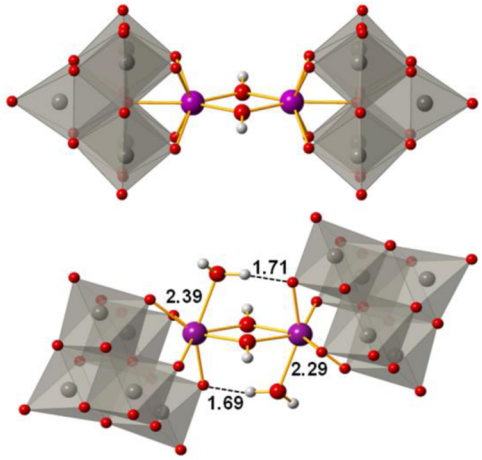

Figure 6. DFT structures and main distances (in Å) for Lindqvist-type dimers $[\{W_5O_{18}Zr(\mu\text{-}OH)\}_2]^{6-}$ (**2L**) and $[\{W_5O_{18}Zr(H_2O)_2(\mu\text{-}OH)\}_2]^{6-}$ (**2L-2H$_2$O**).

Table 3 compares the X-ray data with the computed structures for nonhydrated and -hydrated dimers, showing a general good agreement. Upon water coordination, the most noticeable differences are the flapping of the two POM subunits out of the $\{Zr\text{-}\mu O\}_2$ plane in opposite directions (see Figures 6 and 7), and the shift out of the Zr atom from the POM framework for both the Linqvist- and the Keggin-type dimers. The changes are reflected in the angle between the two Zr atoms and the central position of the POM and in the Zr−O_c distances (see Table 3). Note that the computed Zr−O_c distances are somewhat shorter than the experimental ones for the Keggin dimers, but they reproduce the observed trends, namely, an increase by ∼0.2 Å. Moreover, for hydrated species, we identified intramolecular hydrogen bonds between the H of aqua ligands and the bridging Zr−O−W oxygens of the opposite POM subunit (at ca. 1.7 Å; Figure 6 and 7), which may participate in the stabilization of the dimeric structure. In the case of Lindqvist dimers, none of the proposed X-ray structures contain coordinated water,[7,10] even when the

dx.doi.org/10.1021/ic401999r | Inorg. Chem. 2014, 53, 778−786

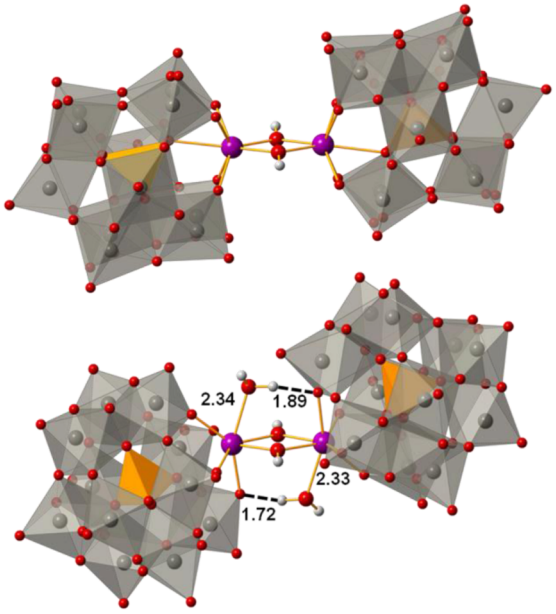

Figure 7. DFT structures and main distances (in Å) for Keggin-type dimers $[\{PW_{11}O_{39}Zr(\mu\text{-}OH)\}_2]^{6-}$ (**2K**) and $[\{PW_{11}O_{39}Zr(H_2O)_2(\mu\text{-}OH)\}_2]^{6-}$ (**2K-2H$_2$O**).

Table 3. Selected Geometrical Parameters in Dimeric Zr-Monosubstituted POMs and Corresponding Dimerization Energies[a]

		X-ray		DFT	
species		nonhydr.	hydr.	nonhydr.	hydr.
Linqvist	Zr···Zr	3.65		3.64	3.69
	Zr-μO	2.14		2.17	2.16
		2.18		2.18	2.16
	Zr−O_w				2.34
	Zr···O_c	2.37		2.38	2.47
	O_c−Zr−Zr	179		178	152
	$\Delta E_{dim.}$			−25.0	−23.9
Keggin	Zr···Zr	3.57	3.57	3.61	3.69
	Zr-μO	2.06	2.13	2.16	2.15
		2.12	2.17	2.17	2.23
	Zr−O_w		2.22		2.34
	Zr···O_c	2.71	2.95	2.52	2.73
	P−Zr−Zr	177	154	167	150
	ΔE_{dim}			−22.8	−23.6

[a]X-ray and computed nonhydrated/hydrated Lindqvist/Keggin dimers. Distances in Å and angles in degrees and dimerization energies, ΔE_{dim}, in kcal mol^{-1}. The X-ray values are taken from refs 7 and 10 for **2L**, ref 11 for **2K**, and ref 12 for **2K−H$_2$O** The geometric parameters are average values. In the case of **2L**, for which two X-ray structures are available (refs 7 and 10), both were averaged.

structure was prepared in aqueous conditions and the crystal contains two H_2O molecules, $(TBA)_6[\{W_5O_{18}Zr(\mu\text{-}OH)\}_2]\cdot 2H_2O$.[7] A plausible explanation could be that the Zr···O_c distances in Lindqvist species are significantly shorter than in Keggin ones (Table 3) disfavoring additional coordination. Nevertheless, we cannot discard uncertainties in X-ray determination due to disordered water positions. In fact, Errington et al. noted the significant crystallographic challenges of these structures.[10] In small Zr^{4+} dimers CPMD calculations showed that the Zr center can be seven- and eight-coordinated in water,[47] whereas in tetramers all Zr centers are eight-coordinated.[54] This means that subtle effects tune the preference for 7-/8-fold coordination of Zr ion. In any case, the results for dimeric structures also strengthen the idea that in aqueous conditions, there is a tendency of Zr atom to bind water molecules and to increase its coordination number.

CONCLUSIONS

We have used static DFT methods with the continuum solvent model IEF-PCM, as well as classical and Car−Parrinello molecular dynamics simulations with the explicit inclusion of solvent water molecules to study the nature of Zr-monosubstituted POMs in water solution at different pH conditions. We analyzed the hydration/dehydration of zirconium center and the protonation/deprotonation at the POM basic centers. Calculations show that in aqueous media, the Zr-monosubstituted monomeric anions tend to have a Zr center with coordination number greater than six, capable to bind up to 3 H_2O molecules. Dimeric species can also coordinate additional water molecules to Zr, which does not seem to affect the dimerization process. Keggin-type structures probably have higher tendency to coordinate additional waters than Lindqvist-type anions because of the longer distance between the Zr and the internal oxygen of the POM that reduces the *coordination number* of the Zr with the POM framework. Furthermore, Car−Parrinello MD simulations show that the position of Zr atom is loose within the oxide POM framework, inducing a flexible coordination environment to the metal ion.

The small thermodynamic preference of $[ZrW_5O_{18}(H_2O)_2]^{2-}$ over $[HZrW_5O_{18}(OH)(H_2O)]^{2-}$ indicates that Zr-hydroxo oxygen is more basic than bridging Zr−O−W oxygen. However, both Zr-aqua and Zr-hydroxo-aqua species could coexist in aqueous solution, and the prevalence of one or the other species might depend on the pH. Simulations of Zr-hydroxo-aqua Lindqvist POM in acidic conditions show that the protonation occurs at the Zr−OH sites, rather than at the Zr−O−W sites. In general, an increase of the acidity of the solution favors the formation of Zr-aqua species, whereas moving to higher pHs, favors the Zr-hydroxo aqua species. Indeed, the simulations at basic conditions show that OH^- deprotonates the aqua ligand to generate hydroxo species. Our findings explain why at high acidic conditions the monomeric species predominate, and the aqua groups are unavailable to act as bridging ligands without further reorganization. On the other hand, alkilination promotes dimeric formation via assembly through Zr-hydroxo moieties. Further work is ongoing in our laboratories to get a more detailed insight into the mechanism of dimerization and assembly of substituted POMs.

ASSOCIATED CONTENT

Supporting Information

RDF plots and the *xyz* coordinates for the most relevant computed structures reported. This material is available free of charge via the Internet at http://pubs.acs.org.

AUTHOR INFORMATION

Corresponding Authors

*E-mail: j.carbo@urv.cat (J.J.C.).
*E-mail: chaumont@unistra.fr (A.C.).

Notes

The authors declare no competing financial interest.

■ ACKNOWLEDGMENTS

We acknowledge support from the Ministerio de Economía y Competitividad (MINECO) of Spain (project CTQ2011−29054-C02−01) and from the Direcció General de Recerca (DGR) of the Autonomous Government of Catalonia Grants 2009SGR462 and XRQTC). A.C. and W.G. thank IDRIS, CINES and UdS for computational support. P.J. carried out this work under the HPC-Europa2 project (hp0063) with the support of the European Commission - Capacities Area - Research Infrastructures.

■ REFERENCES

(1) Cronin, L., Müller, A., Eds.; *Chem. Soc. Rev.* **2012**, *41*, 7325.
(2) (a) Long, D. L.; Tsunashima, R.; Cronin, L. *Angew. Chem., Int. Ed.* **2010**, *49*, 1736. (b) Proust, A.; Thouvenot, R.; Gouzerh, P. *Chem. Commun.* **2008**, 1837. (c) Mizuno, N.; Yamaguchi, K. *Chem. Rec.* **2006**, *6*, 12.
(3) For some specific review on group IV metal-substituted POMs, see: (a) Kholdeeva, O. A.; Maksimovskaya, R. I. *J. Mol. Catal. A: Chem.* **2007**, *262*, 7. (b) Nomiya, K.; Sakai, Y.; Matsunaga, S. *Eur. J. Inorg. Chem.* **2011**, 179. (c) Kholdeeva, O. A. *Eur. J. Inorg. Chem.* **2013**, 1595.
(4) (a) Vanhaecht, S.; Absillis, G.; Parac-Vogt, T. N. *Dalton Trans.* **2012**, *41*, 10018. (b) Absillis, G.; Parac-Vogt, T. N. *Inorg. Chem.* **2012**, *51*, 9902. (c) Ly, T. H. G.; Absillis, G.; Bajpe, S. R.; Martens, J. A.; Parac-Vogt, T. N. *Eur. J. Inorg.* **2013**, 4601. (d) Ly, T. H. G.; Absillis, G.; Parac-Vogt, T. N. *Dalton Trans.* **2013**, *42*, 10929.
(5) Yoshida, S.; Murakami, H.; Sakai, Y.; Nomiya, K. *Dalton Trans.* **2008**, 4630.
(6) Saku, Y.; Sakai, Y.; Nomiya, K. *Inorg. Chim. Acta* **2010**, *363*, 967.
(7) Villanneau, R.; Carabineiro, H.; Carrier, X.; Thouvenot, R.; Herson, P.; Lemos, F.; Ramôa-Ribeiro, F.; Che, M. *J. Phys. Chem. B* **2004**, *108*, 12465.
(8) Chauveau, F.; Éberlé, J.; Lefebvre, J. *Nouv. J. Chim.* **1985**, *9*, 315.
(9) Carabineiro, H.; Villanneau, R.; Carrier, X.; Herson, P.; Lemos, F.; Ramôa Ribeiro, F.; Proust, A.; Che, M. *Inorg. Chem.* **2006**, *45*, 1915.
(10) Errington, R. J.; Petkar, S. S.; Middleton, P. S.; McFarlane, W.; Clegg, W.; Collax, R. A.; Harrington, R. W. *J. Am. Chem. Soc.* **2007**, *129*, 12181.
(11) Kholdeeva, O. A.; Maksimov, G. M.; Maksimovskaya, R. I.; Vanina, M. P.; Trubitsina, T. A.; Naumov, D. Y.; Kolesov, B. A.; Antonova, N. S.; Carbó, J. J.; Poblet, J. M. *Inorg. Chem.* **2006**, *45*, 7224.
(12) Nomiya, K.; Saku, Y.; Yamada, S.; Takahashi, W.; Sekiya, H.; Shinohara, A.; Ishimaru, M.; Sakai, Y. *Dalton Trans.* **2009**, 5504.
(13) (a) Yamaguchi, S.; Kikukawa, Y.; Tsushida, K.; Nakagawa, Y.; Uehara, K.; Yamaguchi, K.; Mizuno, N. *Inorg. Chem.* **2007**, *46*, 8502. (b) Kikukawa, Y.; Yamaguchi, S.; Tsuchida, K.; Nakagawa, Y.; Uehara, K.; Mizuno, N. *J. Am. Chem. Soc.* **2008**, *130*, 5472.
(14) Villanneau, R.; Racimor, D.; Messner-Hening, E.; Rousselière, H.; Picart, S.; Thouvenot, R.; Proust, A. *Inorg. Chem.* **2011**, *50*, 1164.
(15) López, X.; Weinstock, I. A.; Bo, C.; Sarasa, J. P.; Poblet, J. M. *Inorg. Chem.* **2006**, *45*, 6467.
(16) Rustad, J. R.; Casey, W. H. *Nat. Mater.* **2012**, *11*, 223.
(17) (a) Wang, J.; Rustad, J. R.; Casey, W. H. *Inorg. Chem.* **2007**, *46*, 2962. (b) Rustad, J. R. *Geochim. Cosmochim. Acta* **2005**, *69*, 4397. (c) Rustad, J. R.; Loring, J. S.; Casey, W. H. *Geochim. Cosmochim. Acta* **2004**, *68*, 3011.
(18) (a) Villa, E. M.; Ohlin, C. A.; Casey, W. H. *J. Am. Chem. Soc.* **2010**, *132*, 5264. (b) Villa, E. M.; Ohlin, C. A.; Rustad, J. R.; Casey, W. H. *J. Am. Chem. Soc.* **2009**, *131*, 16488. (c) Villa, E. M.; Ohlin, C. A.; Balogh, E.; Anderson, T. M.; Nyman, M. D.; Casey, W. H. *Angew. Chem., Int. Ed.* **2008**, *47*, 48477.
(19) (a) López, X.; Miró, P.; Carbó, J. J.; Rodríguez-Fortea, A.; C. Bo, C.; Poblet, J. M. *Theor. Chem. Acc.* **2011**, *128*, 393. (b) López, X.; Carbó, J. J.; Bo, C.; Poblet, J. M. *Chem. Soc. Rev.* **2012**, *41*, 7537.
(20) Frisch, M. J.; Trucks, G. W.; Schlegel, H. B.; Scuseria, G. E.; Robb, M. A.; Cheeseman, J. R.; Scalmani, G.; Barone, V.; Mennucci, B.; Petersson, G. A.; Nakatsuji, H.; Caricato, M.; Li, X.; Hratchian, H. P.; Izmaylov, A. F.; Bloino, J.; Zheng, G.; Sonnenberg, J. L.; Hada, M.; Ehara, M.; Toyota, K.; Fukuda, R.; Hasegawa, J.; Ishida, M.; Nakajima, T.; Honda, Y.; Kitao, O.; Nakai, H.; Vreven, T.; Montgomery, Jr., J. A.; Peralta, J. E.; Ogliaro, F.; Bearpark, M.; Heyd, J. J.; Brothers, E.; Kudin, K. N.; Staroverov, V. N.; Kobayashi, R.; Normand, J.; Raghavachari, K.; Rendell, A.; Burant, J. C.; Iyengar, S. S.; Tomasi, J.; Cossi, M.; Rega, N.; Millam, N. J.; Klene, M.; Knox, J. E.; Cross, J. B.; Bakken, V.; Adamo, C.; Jaramillo, J.; Gomperts, R.; Stratmann, R. E.; Yazyev, O.; Austin, A. J.; Cammi, R.; Pomelli, C.; Ochterski, J. W.; Martin, R. L.; Morokuma, K.; Zakrzewski, V. G.; Voth, G. A.; Salvador, P.; Dannenberg, J. J.; Dapprich, S.; Daniels, A. D.; Farkas, Ö.; Foresman, J. B.; Ortiz, J. V.; Cioslowski, J.; Fox, D. J. *Gaussian 09*, Revision A.1; Gaussian, Inc.: Wallingford, CT, 2009.
(21) (a) Lee, C.; Yang, C.; Parr, R. G. *Phys. Rev. B* **1988**, *37*, 785. (b) Becke, A. D. *J. Chem. Phys.* **1993**, *98*, 5648. (c) Stephens, P. J.; Devlin, F. J.; Chabalowski, C. F.; Frisch, M. J. *J. Phys. Chem.* **1994**, *98*, 11623.
(22) Hay, P. J.; Wadt, W. R. *J. Chem. Phys.* **1985**, *82*, 270.
(23) (a) Francl, M. M.; Pietro, W. J.; Hehre, W. J.; Binkley, J. S.; Gordon, M. S.; Defrees, D. J.; Pople, J. A. *J. Chem. Phys.* **1982**, *77*, 3654. (b) Hehre, W. J.; Ditchfield, R.; Pople, J. A. *J. Chem. Phys.* **1972**, *56*, 2257. (c) Hariharan, P. C.; Pople, J. A. *Theor. Chim. Acta* **1973**, *28*, 213.
(24) Cances, E.; Mennucci, B.; Tomasi, J. *J. Chem. Phys.* **1997**, *107*, 3032.
(25) (a) Chaumont, A.; Wipff, G. *Phys. Chem. Chem. Phys.* **2008**, *10*, 6940. (b) Chaumont, A.; Wipff, G. *J. Phys. Chem. C* **2009**, *113*, 18233. (c) Chaumont, A.; Wipff, G. *C. R. Chim.* **2012**, *15*, 107. (d) Chaumont, A.; Wipff, G. *Eur. J. Inorg. Chem.* **2013**, 1835.
(26) Case, D. A.; Darden, T. A.; Cheatham, T. E.; Simmerling, C. L.; Wang, J.; Duke, R. E.; Luo, R.; Crowley, R.; Walker, R. C. Zhang, W.; Merz, K. M.; Wang, B.; Hayik, S.; Roitberg, A.; Seabra, G.; Kolossvary, I.; Wong, K. F.; Paesani, F.; Vanicek, J.; Wu, X.; Brozell, S. R.; Steinbrecher, T.; Gohlke, H.; Yang, L.; Tan, C.; Mongan, J.; Hornak, V.; Cui, G.; Seetin, M. G.; Sagui, C.; Babin, V.; Kollman, P. A. *AMBER 10*; University of California: San Francisco, CA, 2008.
(27) Case, D. A.; Darden, T. A.; Cheatham, T. E.; Simmerling, C. L.; Wang, J.; Duke, R. E.; Luo, R.; Walker, R. C.; Zhang, W.; Merz, K. M.; Roberts, B.; Wang, B.; Hayik, S.; Roitberg, A.; Seabra, G.; Kolossvai, I.; Wong, K. F.; Paesani, F.; Vanicek, J.; Liu, J.; Wu, X.; Brozell, S. R.; Steinbrecher, T.; Gohlke, H.; Cai, Q.; Ye, X.; Wang, J.; Hsieh, M. J.; Cui, G.; Roe, D. R.; Mathews, D. H.; Seetin, M. G.; Sagui, C.; Babin, V.; Luchko, T.; Gusarov, S.; Kovalenko, A.; Kollman, P. A. *AMBER 11*; University of California: San Francisco, CA, 2008.
(28) (a) López, X.; Nieto-Draghi, C.; Bo, C.; Bonet-Avalos, J.; Poblet, J. M. *J. Phys. Chem. A* **2005**, *109*, 1216. (b) Leroy, F.; Miró, P.; Poblet, J. M.; Bo, C.; Bonet-Ávalos, J. *J. Phys. Chem. B* **2008**, *112*, 8591.
(29) (a) Becke, A. D. *Phys. Rev. A* **1988**, *38*, 3098. (b) Perdew, J. P. *Phys. Rev. B* **1986**, *33*, 8822.
(30) (a) Klamt, A. J.; Schüürmann, G. J. *J. Chem. Soc., Perkin. Trans.* **1993**, *2*, 799. (b) Andzelm, J.; Kölmel, C.; Klamt, A. J. *Chem. Phys.* **1995**, *103*, 9312. (c) Klamt, A. J. *Chem. Phys.* **1995**, *99*, 2224.
(31) Baerends, E. J.; Ziegler, T.; Autschbach, J.; Bashford, D.; Bérces, A.; Bickelhaupt, F. M.; Bo, C.; Boerrigter, P. M.; Cavallo, L.; Chong, D. P.; Deng, L.; Dickson, R. M.; Ellis, D. E.; van Faassen, M.; Fan, L.; Fischer, L.; Fonseca Guerra, C.; Ghysels, A.; Giammona, A.; van Gisbergen, S. J. A.; Götz, A. W.; Groeneveld, J. A.; Gritsenko, O. V.; Grüning, M.; Gusarov, S.; Harris, F. E.; van den Hoek, P.; Jacob, C. R.; Jacobsen, H.; Jensen, L.; Kaminski, J. W.; van Kessel, G.; Kootstra, F.; Kovalenko, A.; Krykunov, M. V.; van Lenthe, E.; McCormack, D. A.; Michalak, A.; Mitoraj, M.; Neugebauer, J.; Nicu, V. P.; Noodleman, L.; Osinga, V. P.; Patchkovskii, S.; Philipsen, P. H. T.; Post, D.; Pye, C. C.; Ravenek, W.; Rodríguez, J. I.; Ros, P.; Schipper, P. R. T.; Schreckenbach, G.; Seldenthuis, J. S.; Seth, M.; Snijders, J. G.; Solà, M.; Swart, M.; Swerhone, G.; te Velde, G.; Vernooijs, P.; Versluis, L.; Visscher, L.; Visser, O.; Wang, F.; Wesolowski, T. A.; van Wezenbeek, E. M.; Wiesenekker, G.; Wolff, S. K.; Woo, T. K.; Yakovlev, A. L.; Baerends, J. E. *ADF2011*; SCM: Amsterdam, The Netherlands, 2011.

(32) (a) Baerends, E. J.; Ellis, D. E.; Ros, P. *Chem. Phys.* **1973**, *2*, 41. (b) Versluis, L.; Ziegler, T. J. *Chem. Phys.* **1988**, *88*, 322. (c) te Velde, G.; Baerends, E. J. J. *Comput. Phys.* **1992**, *99*, 84. (d) Fonseca-Guerra, C. J.; Snijders, G.; te Velde, G.; Baerends, E. J. *Theor. Chem. Acc.* **1998**, *99*, 391.
(33) Rappé, A. K.; Casewit, C. J.; Colwell, K. S.; Goddard, W. A., III; Skifff, W. M. *J. Am. Chem. Soc.* **1992**, *114*, 10024.
(34) Aqvist, J. *J. Phys. Chem.* **1990**, *94*, 8021.
(35) Baaden, M.; Burgard, M.; Wipff, G. *J. Phys. Chem. B* **2001**, *105*, 11131.
(36) Jorgensen, W. L.; Chandrasekhar, J.; Madura, J. D.; Impey, R. W.; Klein, M. L. *J. Chem. Phys.* **1983**, *79*, 926.
(37) Darden, T. A.; York, D. M.; Pedersen, L. G. *J. Chem. Phys.* **1993**, *98*, 10089.
(38) Berendsen, H. J. C.; Postma, J. P. M.; van Gunsteren, W. F.; DiNola, A. *J. Chem. Phys.* **1984**, *81*, 3684.
(39) *CPMD*; IBM Corp.: Armonk, NY, 1990−2006; MPI für Festkörperforschung, Stuttgart, Germany, 1997−2001.
(40) Troullier, N.; Martins, J. L. *Phys. Chem. Rev. B* **1991**, *43*, 1993.
(41) Louie, S. G.; Froyen, S.; Cohen, M. L. *Phys. Rev. B* **1982**, *26*, 1738.
(42) (a) Vilà-Nadal, L.; Rodríguez-Fortea, A.; Yan, L.-K.; Wilson, E. F.; Poblet, J. M. *Angew. Chem., Int. Ed.* **2009**, *48*, 1. (b) Rodríguez-Fortea, A.; Vilà-Nadal, L.; Poblet, J. M. *Inorg. Chem.* **2008**, *47*, 7745.
(43) (a) Becke, A. D. *Phys. Rev. A.* **1988**, *38*, 3098. (b) Becke, A. D. *Phys. Rev. A* **1988**, *38*, 3098.
(44) Buhl, M.; Parrinello, M. *Chem.—Eur. J.* **2001**, *7*, 4487.
(45) (a) Nosé, S. *J. Chem. Phys.* **1984**, *81*, 511. (b) Hoover, W. G. 1985, *31*, 1695
(46) Hagfeldt, C.; Kessler, V.; Persson, I. *Dalton Trans.* **2004**, 2142 and references therein.
(47) Messner, C. B.; Hofer, T. S.; Randolf, B. R.; Rode, B. M. *Phys. Chem. Chem. Phys.* **2011**, *13*, 224.
(48) (a) Antonova, N. S.; Carbó, J. J.; Kortz, U.; Kholdeeva, O. A.; Poblet, J. M. *J. Am. Chem. Soc.* **2010**, *132*, 7488. (b) Donoeva, B. G.; Trubitsina, T. A.; Antonova, N. S.; Carbó, J. J.; Poblet, J. M.; Al-Kadamany, G.; Kortz, U.; Kholdeeva, O. A. *Eur. J. Inorg. Chem.* **2010**, 5312. (c) Jiménez-Lozano, P.; Ivanchikova, I. D.; Kholdeeva, O. A.; Poblet, J. M.; Carbó, J. J. *Chem. Commun.* **2012**, *48*, 9266.
(49) Sadoc, A.; Messaudi, S.; Furet, E.; Gautier, R.; Le Fur, E.; Le Polles, L.; Pivan, J. *Inorg. Chem.* **2007**, *46*, 4835.
(50) (a) Buhl, M.; Diss, R.; Wipff, G. *J. Am. Chem. Soc.* **2005**, *127*, 13506. (b) Buhl, M.; Kabrede, H.; Diss, R.; Wipff, G. *J. Am. Chem. Soc.* **2006**, *128*, 6357.
(51) Because of computational limitations, we had to define a relatively small solvent box around the POM. Consequently, we can only simulate high acidic or basic pHs. For acidic conditions within a cubix box of 16.3 $Å^3$, the pHs are −0.1 and 0.4 for **3** and **1** H_3O^+, respectively. For basic conditions within a box of 17.8 $Å^3$, the pHs are 13.9 and 13.5 for **3** and **1** OH^-, respectively.
(52) Rao, N.; Holerca, M. N.; Pophristic, V. *J. Chem. Theory Comput.* **2008**, *4*, 145.
(53) See for example: Falvello, L. R.; Gines, J. C.; Carbó, J. J.; Lledós, A.; Navarro, R.; Soler, T.; Urriolabeitia, E. P. *Inorg. Chem.* **2006**, *45*, 6803.
(54) Rao, N.; Holerca, M. N.; Klein, M. L.; Pophristic, V. *J. Phys. Chem. A* **2007**, *111*, 11395.